As an example, Fig. 4 shows the results obtained for the mixed-potential Green's functions in Fig. 3(a) obtained with (9), as compared with the Green's functions obtained using a standard Sommerfeld formulation (10) of the identical problem in Fig. 3(b). Fig. 4 shows the comparison for both the electric scalar potential and magnetic vector potential (analogous to the electric scalar potential, but not vanishing in the walls), when the source is placed at points A and B in Fig. 3, and as a function of the position of the observer point. As we observe, the agreement is excellent; therefore, validating the parallel-plate Green's functions computed with the new algorithm.

V. Conclusions

In this paper, a new and efficient technique for the convergence acceleration of a large class of series arising in electromagnetic problems has been presented. The technique can be viewed as the successive application of the integration-by-parts technique to discrete sequences; therefore, the given name of the "summation-by-parts technique."

The technique has been first applied to the numerical evaluation of a simple canonical series, showing that convergence is greatly enhanced, allowing to obtain very small relative errors with just a few operations. The technique described can be applied to many real electromagnetic problems and, in this paper, it has been used for the efficient numerical calculation of the parallel-plate mixed-potential Green's functions.

References

[1] C. J. Railton and S. A. Meade, "Fast rigorous analysis of shielded planar filters," *IEEE Trans. Microwave Theory Tech.*, vol. 40, pp. 978–985, May 1992.

[2] J. Y. Lee, T. S. Horng, and N. G. Alexopoulos, "Analysis of cavity-backed aperture antennas with a dielectric overlay," *IEEE Trans. Antennas Propagat.*, vol. 42, pp. 1556–1562, Nov. 1994.

[3] A. A. Maradudin and A. R. McGurn, "Photonic band structures of two-dimensional dielectric media," in *Photonic Band Gaps and Localization*. ser. NATO ASI series, C. M. Soukoulis, Ed. New York: Plenum, 1993, pp. 247–268.

[4] C. Brezinski and M. R. Zaglia, *Extrapolation Methods*. Amsterdam, The Netherlands: Elsevier, 1991.

[5] N. Kinayman and M. I. Aksun, "Comparative study of acceleration techniques for integrals and series in electromagnetic problems," *Radio Sci.*, vol. 30, pp. 1713–1722, Nov.–Dec. 1995.

[6] Y. L. Chow, J. J. Yang, D. G. Fang, and G. E. Howard, "A closed-form spatial Green's function for the thick microstrip substrate," *IEEE Trans. Microwave Theory Tech.*, vol. 39, pp. 588–592, Mar. 1991.

[7] G. V. Eleftheriades, J. R. Mosig, and M. Guglielmi, "A fast integral equation technique for shielded planar circuits defined on nonuniform meshes," *IEEE Trans. Microwave Theory Tech.*, vol. 44, pp. 2293–2296, Dec. 1996.

[8] G. G. Gentili, L. E. Garcia-Castillo, M. Salazar-Palma, and F. Perez-Martinez, "Green's function analysis of single and stacked rectangular microstrip patch antennas enclosed in a cavity," *IEEE Trans. Antennas Propagat.*, vol. 45, pp. 573–579, Apr. 1997.

[9] M. J. Park and S. Nam, "Rapid calculation of the Green's function in the shielded planar structures," *IEEE Microwave Guided Wave Lett.*, vol. 7, pp. 326–328, Oct. 1997.

[10] I. S. Gradshteyn and I. M. Ryzhik, *Table of Integrals, Series, and Products*. New York: Academic, 1965.

[11] A. Alvarez-Melcón and J. R. Mosig, "Two techniques for the efficient numerical calculation of the Green's functions for planar shielded circuits and antennas," *IEEE Trans. Microwave Theory Tech.*, vol. 48, pp. 1492–1504, Sept. 2000.

[12] J. J. Yang, Y. L. Chow, G. E. Howard, and D. G. Fang, "Complex images of an electric dipole in homogeneous and layered dielectrics between two ground planes," *IEEE Trans. Microwave Theory Tech.*, vol. 40, pp. 595–600, Mar. 1992.

[13] J. R. Mosig, "Integral equation technique," in *Numerical Techniques for Microwave and Millimeter-Wave Passive Structures*, T. Itoh, Ed. New York: Wiley, 1989, ch. 3, pp. 133–213.

[14] M.-J. Tsai, C. Chen, and N. G. Alexopoulos, "Sommerfeld integrals in modeling interconnects and microstrip elements in multi-layered media," *Electromagnetics (Special Issue)*, vol. 18, no. 3, pp. 267–288, 1998.

Direct Extraction of Linear HBT-Model Parameters Using Nine Analytical Expression Blocks

Achour Ouslimani, Jean Gaubert, Habiba Hafdallah, Ahmed Birafane, Pierre Pouvil, and H. Leier

***Abstract*—A method to determine the heterojunction bipoloar transistor (HBT) equivalent-circuit elements without numerical optimizations is presented. It is based on the extraction of nine analytical expressions, which are referred to here as "blocks." The model elements are extracted using certain blocks for some of them and three nonlinear equations derived from a combination of four expression blocks for some others. The base and collector resistances can be determined at each bias point. The method is validated treating the on-wafer HBTs.**

***Index Terms*—Analytical method, heterojunction bipolar transistor, parameter extraction.**

I. Introduction

An accurate parameter-extraction procedure of the linear equivalent circuit is crucial to optimize the device and circuit performances. Approaches that consist of reducing the number of unknown elements by using complementary characterizations for independently estimating as many heterojunction bipolar transistor (HBT) parameters as possible have been proposed [1]–[3]. Measurements of special test structures and geometrical and material parameters are needed in [1] to obtain some of the parasitic parameter values. The measurements of two separate test structures are proposed in [2] and [3] to determine the probe-pattern parasitic. The cutoff mode measurements are used in [2] to determine some of the HBTs' capacitances, and the equivalent circuit of the device biased to active mode is obtained using numerical optimizations. Analytical expressions and numerical optimizations are used in [3] and [4] and the information about the geometry device is used to evaluate the ratio μ between the extrinsic and intrinsic base–collector capacitances. Analytical extraction methods have been proposed in [5] and [6]. In [5], the method is based on the use of local fitting routines and certain assumptions. In [6], the S-parameters measured under open-collector condition are used to determine the extrinsic elements. An approach based on both empirical optimization and analytical evaluations is reported in [7]. Initial values of HBT parameters are estimated from dc and multibias S-parameter measurements and then used to achieve the evaluation of the HBT model elements by the impedance-block conditioned optimization. Finally, a procedure combining the analytical and optimization approaches was developed in [8], in which the influence of pad capacitances is discussed.

Manuscript received May 1, 2000; revised October 20, 2000.

A. Ouslimani, J. Gaubert, H. Hafdallah, A. Birafane, and P. Pouvil are with the Ecole Nationale Supérieure de l'Electronique et de ses Applications, 95014 Cergy Pontoise, France.

H. Leier is with the Daimler Benz Research Center, D-7900 Ulm, Germany

Publisher Item Identifier S 0018-9480(02)00019-4.

We present a new analytical method of parameter extraction. It is based on the obtainment of suitable organization of combined Z-parameter analytical expressions. Each analytical expression is structured to obtain a polynomial function with ω as variable and whose coefficients depend only on the circuit elements. The polynomial functions are analyzed in order to choose the most adequate coefficients, referred to here as "blocks" ($b1$–$b9$, as shown in Table I). The model elements are calculated using certain blocks for some of them and three nonlinear equations for some others. In particular, the base and collector resistances considered bias independent in the previous methods can be obtained here at each bias point with the other HBT bias dependent elements. The parasitic inductances are determining taking into account the influence of the inductive terms due to other HBT parameters. The effect of base–contact impedance as modeled in [1] is very visible in low-frequency range and, therefore, its contribution is taken into account. The procedure is validated treating GaInP/GaAs and GaInP/InP HBTs. In this investigation, the procedure is applied to extract the circuit parameters of a GaInP/GaAs HBT.

II. Theory of Parameter-Extraction Procedure

The combined expressions of Z-parameters of the equivalent circuit shown in Fig. 1 can be expressed as follows without approximations:

$$Z_{11}-Z_{12}=Z_b+\frac{(Z_\pi+R_b)g_0+j\omega C_{bc}R_b+j\omega C_cR_bA}{Y}+j\omega L_b \tag{1}$$

$$Z_{22}-Z_{12}=R_c+\frac{1}{Y}+j\omega L_c \tag{2}$$

$$Z_{12}-Z_{21}=\frac{g_mZ_\pi}{Y} \tag{3}$$

with $Z_\pi=(R_\pi)/(1+j\omega R_\pi C_\pi)$, $C=(C_{bc}C_c)/(C_{bc}+C_c)$, $Y=j\omega(C_{bc}+C_c)(1+j\omega CR_b)A+g_0(1+j\omega C_{bc}R_b)$, $A=1+(g_0+g_m)Z_\pi$, and $g_m=g_{m0}e^{-j\omega\tau_d}$, where g_{m0} is the dc transconductance. The structured polynomial functions are obtained from (1)–(3) using the hypothesis summarized in Table II, and as shown in (4)–(12), at the bottom of this page, with $R_e=(R_\pi)/(1+g_{m0}R_\pi)$

TABLE I
Analytical Expressions of the Blocks. The Values for $V_{CE}=2$ V, $I_B=150$ mA: $b1=55\ \Omega$, $b2=1410^{-6}$ S, $b3=58.2\ \Omega$, $b4=34$ fF, $b5=26\ \Omega$, $b6=168$ pH, $b7=58.9$, $b8=20\ \Omega$, $b9=58.2$ pH

$b1=R_c+\frac{R_eC_\pi}{(C_{bc}+C_c)}$	$b2=\frac{g_0}{g_{m_o}R_\pi}$ $\quad b3=\frac{R_bC+R_eC_\pi}{(C_{bc}+C_c)}$
$b4=C_{bc}+C_c$	$b5=\frac{R_bC}{C_{bc}}+g_0\frac{R_bR_eC_\pi}{(C_{bc}+C_c)}$
$b6=L_e+\frac{R_eC_\pi R_bC_{bc}}{(C_{bc}+C_c)}$	$b7=g_{m0}R_\pi+1$
$b8=R_E+R_e+\frac{R_bC_{bc}}{(g_{m_o}R_\pi+1)(C_{bc}+C_c)}$	
$b9=\frac{R_cC_\pi}{C_{bc}+C_c}(R_eC_\pi+R_bC-\tau_d)-L_c$	

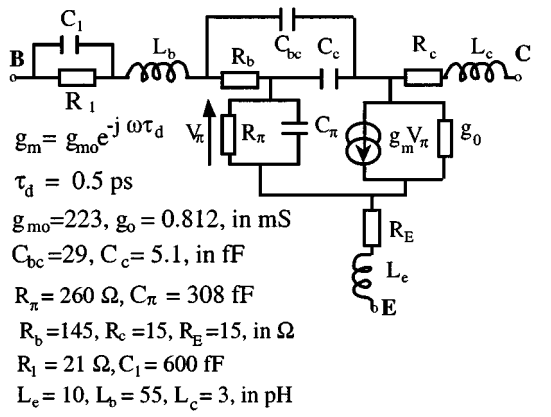

Fig. 1. HBT linear equivalent circuit.

III. Extraction of the Circuit Parameters

The S-parameter measurements are performed from 0.3 to 40 GHz and converted to Z-parameters to determine R_1, C_1, and the nine blocks. The resistance R_E and the ideality factor N_E are extracted from block 8 measured at different emitter currents. The inductances

$$\mathrm{Real}(Z_{22}-Z_{12})=\frac{g_0}{(g_{m0}R_\pi+1)^2(C_{bc}+C_c)^2\omega^2}+b1-\frac{R_eC_\pi R_bC}{(C_{bc}+C_c)}(R_eC_\pi-\tau_d)\omega^2 \tag{4}$$

$$\mathrm{Real}\left(\frac{1}{Z_{12}-Z_{21}}\right)=b2-(C_{bc}+C_c)(R_eC_\pi+R_bC)\omega^2 \tag{5}$$

$$\mathrm{Real}(Z_{21}-Z_{12})=\frac{-g_0}{(g_{m0}R_\pi+1)(C_{bc}+C_c)^2\omega^2}+b3+\tau_d\frac{R_bC(R_eC_\pi-\tau_d)\omega^2}{(C_{bc}+C_c)} \tag{6}$$

$$\mathrm{Imag}\left(\frac{1}{Z_{12}-Z_{21}}\right)=b4\omega-\Big[\tau_d(R_eC_\pi-\tau_d)+R_eC_\pi R_bC\Big](C_{bc}+C_c)\omega^3 \tag{7}$$

$$\mathrm{Real}(Z_{11}-Z_{12})=\frac{R_1}{1+(R_1C_1\omega)^2}+b5 \tag{8}$$

$$\mathrm{Imag}(Z_{12})=g_0\frac{\Big[R_\pi(C_{bc}+C_c)-R_bC_{bc}\Big]}{(g_{m0}R_\pi+1)^2(C_{bc}+C_c)^2}\frac{1}{\omega}+b6\omega-\left(\frac{R_eC_\pi R_bC_{bc}}{C_{bc}+C_c}+R_eR_bC\right)(R_eC_\pi-\tau_d)R_bC\omega^3 \tag{9}$$

$$\frac{-\mathrm{Imag}(Z_{21})}{\mathrm{Imag}(Z_{22}-Z_{12})}=b7\frac{1+\Big[L_e(C_{bc}+C_c)+R_eC_\pi R_bC_{bc}-\tau_d(R_eC_\pi+R_bC-\tau_d)\Big]\omega^2}{1+\Big[-L_c(g_{m0}R_\pi+1)(C_{bc}+C_c)+R_\pi C_\pi(R_eC_\pi+R_{bC}-\tau_d)\Big]\omega^2} \tag{10}$$

$$\mathrm{Real}(Z_{12})=b8+\frac{R_bC_{bc}R_eC_\pi}{C_{bc}+C_c}(R_eC_\pi+R_bC-\tau_d)\omega^2 \tag{11}$$

$$-\omega\mathrm{Imag}(Z_{22}-Z_{12})=\frac{1}{(g_{m0}R_\pi+1)(C_{bc}+C_c)}+b9\,\omega^2-b9\Big[(R_bC)^2+(R_eC_\pi-\tau_d)^2\Big]\omega^4 \tag{12}$$

TABLE II
HYPOTHESIS AND HYPOTHESIS NUMBER $H_i (i = 1 to 4)$. AS AN EXAMPLE, (9)–(13) AND (16) ARE OBTAINED USING H_1 AND H_2 HYPOTHESIS

hypothesis	H_i
$g_0 R_e C_\pi << C_{bc} + C_c$	
$g_0 R_e C_\pi R_b C_{bc} << (C_{bc} + C_c)(R_e C_\pi + R_b C - \tau_d$	H_1
$\frac{g_{m0} R_\pi}{g_{m0} R_\pi + 1} \approx 1$, $f << \frac{1}{2\pi\tau_d}$, $\frac{g_0 \tau_d}{g_{m0} R_\pi + 1} << C_{bc} + C_c$	H_2
$\frac{g_0 R_e C_\pi R_b C_{bc}}{(g_{m0} R_\pi + 1)(C_{bc} + C_c)^2} << R_e + R_E$	
$\frac{g_0 R_e R_b C}{(g_{m0} R_\pi + 1)(C_{bc} + C_c)} << R_e + R_E$	H_3
$\frac{R_e C_\pi + R_b C - \tau_d}{g_{m0} R_\pi + 1} << R_e C_\pi$	H_4

Equation (s)	eq.4	eqs. 5-9, 12	eq.10	eq.11
H_i used	H_1, H_2, H_4	H_1, H_2	H_1	H_1,H_2, H_3

are obtained taking into account the influence of the inductive terms. Blocks 2 and 7 are used to determine g_{m0} and g_0. The parameters C_π, C_{bc}, C_c, R_b, R_c, and τ_d are obtained using three nonlinear equations. The pad capacitances (not shown in Fig. 1) are removed from measurements.

A. Determination of the Value of Each Block ($bi, i = 1$–9)

The values of the nine blocks can be extracted using the frequency dependence of the left members in (4)–(12). Each block value is obtained using linear regression over an adequate frequency range (Table III). As an example, the values $b1$ and $b5$ are extracted using the frequency dependencies of $\mathrm{Real}(Z_{22} - Z_{12})$ and $\mathrm{Real}(Z_{11} - Z_{12})$, respectively [see Fig. 2(a) and (b)]. These resullts confirm the theoretical evolution described in (4) and (8). The first term of the right-hand-side expression in (4) describes the fast decrease of $\mathrm{Real}(Z_{22} - Z_{12})$ in the low-frequency range. The second term has a constant value $b1$ over all frequencies $fb1_1 = 0.3$ GHz $\ll f \ll fb1_2 = 254$ GHz. Thereby $b1$ can be easily extracted. In Fig. 2(b), $\mathrm{Real}(Z_{11} - Z_{12})$ decreases quickly for $f \leq 20$ GHz and becomes frequency independent for $f > 20$ GHz. These experimental evolution is well described in (8) and allows us to extract $b5$.

B. Determination of R_1, C_1, R_E, and the Access Inductances

Fig. 2(b) and (8) are used to determine R_1 and C_1 as follows:

$$m_1 - b5 = \frac{R1}{1 + (R_1 C_1 f_1)^2}$$

and

$$m_2 - b5 = \frac{R1}{1 + (R_1 C_1 f_2)^2} \tag{13}$$

where m_1 and m_2 are the values of $\mathrm{Real}(Z_{11} - Z_{12})$ corresponding to f_1 and f_2, respectively. Frequencies f_1 and f_2 are chosen over a frequency range where the influence of the first term in (8) is important compared to that of the second term. Using (13), we have

$$R_1 = (m_1 - b5)\left(1 + \frac{1 - \dfrac{m_1 - b5}{m_2 - b5}}{\dfrac{m_1 - b5}{m_2 - b5} - \left(\dfrac{f_2}{f_1}\right)^2}\right)$$

TABLE III
FREQUENCY RANGE WHERE EACH BLOCK VALUE IS EXTRACTED

bi	freqency range
b1	$f >> f_{b1_1} = \frac{1}{2\pi}\sqrt{\frac{g_0 / [(g_{m0} R_\pi + 1)^2 (C_{bc} + C_c)]}{R_c (C_{bc} + C_c) + R_e C_\pi}}$
	$f << f_{b1_2} = \frac{1}{2\pi}\sqrt{\frac{R_c (C_{bc} + C_c) + R_e C_p}{R_b C R_e C_p (R_e C_p - \tau_d)}}$
b2	$f << f_{b2} = \frac{1}{2\pi}\sqrt{g_0 [g_{m0} R_\pi (C_{bc} + C_c)(R_e C_\pi + R_b C)]^{-1}}$
b3	$f >> f_{b3_1} = \frac{1}{2\pi}\sqrt{\frac{g_0 / [(g_{m0} R_\pi + 1)(C_{bc} + C_c)]}{R_e C_\pi + R_b C}}$
	$f << f_{b3_2} = \frac{1}{2\pi}\sqrt{\frac{R_b C + R_e C_\pi}{\tau_d R_b C (R_e C_\pi - \tau_d)}}$
b4	$f << f_{b4} = \frac{1}{2\pi}\sqrt{[\tau_d (R_e C_\pi - \tau_d) + R_e C_\pi R_b C]^{-1}}$
b5	$1 + (R_1 C_1 2\pi f)^2 >> \frac{R_1}{\frac{g_0 R_b R_e C_\pi}{C_{bc} + C_c} + \frac{R_b C}{C_{bc}}}$
b6	$f >> f_{b6_1} = \frac{1}{2\pi}\sqrt{\frac{g_0 [R_\pi (C_{bc} + C_c) - R_b C_{bc}] g_{m0} R_\pi + 1)^{-2}}{(C_{bc} + C_c)[L_e (C_{bc} + C_c) + R_e C_\pi R_b C_{bc}]}}$
	$f << f_{b6_2} = \frac{1}{2\pi}\sqrt{\frac{[L_e (C_{bc} + C_c) + R_e C_\pi R_b C_{bc}](R_e C_\pi - \tau_d)^{-1}}{R_b C (R_e R_b C (C_{bc} + C_c) + R_e C_\pi R_b C_{bc})}}$
b7	$f << f_{b7_1} = \frac{1}{2\pi}\sqrt{[L_e (C_{bc} + C_c) + R_e C_\pi R_b C_{bc} - \tau_d (R_e C_\pi + R_b C - \tau_d)]^{-1}}$
	$f << f_{b7_2} = \frac{1}{2\pi}\sqrt{[-L_c (C_{bc} + C_c)(g_{m0} R_\pi + 1) + R_\pi C_\pi (R_e C_\pi + R_b C - \tau_d)]^{-1}}$
b8	$f << f_{b8} = \frac{1}{2\pi}\sqrt{\frac{(R_E + R_e)(C_{bc} + C_c) + \frac{R_b C_{bc}}{g_{m_0} R_\pi + 1}}{R_b C_{bc} R_e C_\pi (R_e C_\pi + R_b C - \tau_d)}}$
b9	$f << f_{b9} = \frac{1}{2\pi}\sqrt{\frac{1}{(R_b C)^2 + (R_e C_\pi - \tau_d)^2}}$

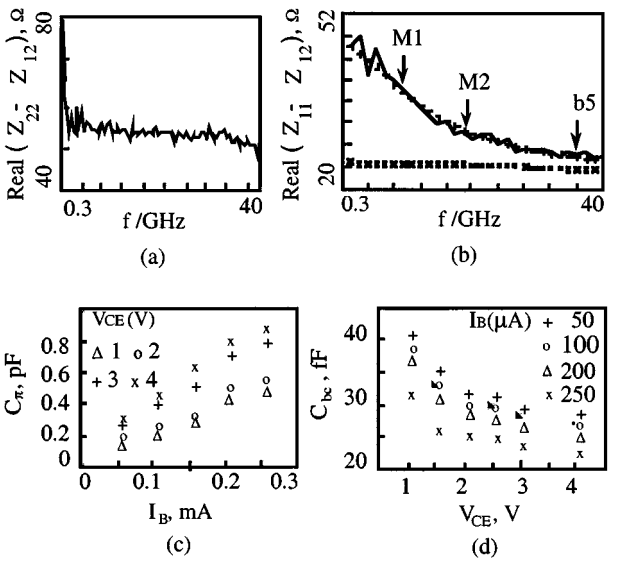

Fig. 2. Determination of: (a), (b) $b1$ and $b5$; R_1, $C_1(b)$. $\mathrm{Real}(Z_{11} - Z_{12})$: measured (−), simulated with R_1, C_1, (++), simulated without R_1, C_1 (××). (c), (d) HBTs capacitances versus bias.

$$C_1 = \frac{1}{R_1}\sqrt{\frac{1 - \dfrac{m_1 - b5}{m_2 - b5}}{(2\pi f_1)^2\left[\dfrac{m_1 - b5}{m_2 - b5} - \left(\dfrac{f_2}{f_1}\right)^2\right]}} \tag{14}$$

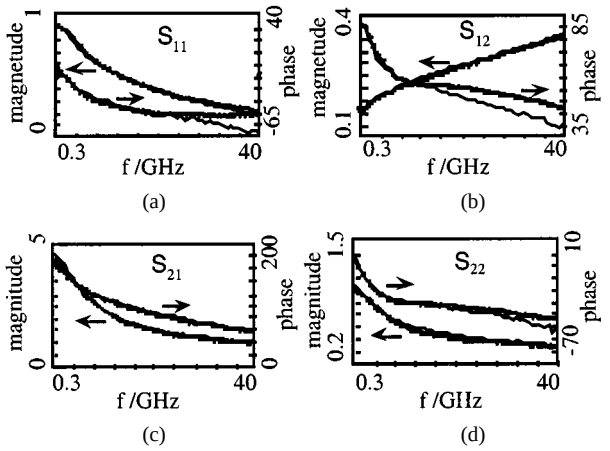

Fig. 3. Measured $(--)$ and simulated $(+++)$ S-parameters.

with ($f_1 = 6.652$ GHz, $m_1 = 41.71\ \Omega$) and ($f_2 = 19.356$ GHz, $m_2 = 31.25\ \Omega$) corresponding to points $M1$ and $M2$, respectively, we have $R_1 = 21.5\ \Omega$ and $C_1 = 0.6$ pF.

The resistance R_E is determined using block 8 measured over a low-frequency range $f \ll f_{b8}$ at different emitter currents I_E, such as in [9]. The parasitic inductances are determined from S-parameters measured in a nonconducting state and taking into account the influence of the inductive terms due to certain device parameters that contribute to increase the global inductive effect of the transistor [10].

C. Determination of R_π, g_{m0}, and g_0

R_π is determined from well-known theoritical expression $R_\pi = (N_E V_T)/(I_B)$, and g_{m0} and g_0 are determined using block 7 and block 2, respectively: $g_{m0} = (b7 - 1)/R_\pi$ and $g_0 = b2 g_{m0} R_\pi$.

D. Determination of C_π, C_{bc}, R_b, R_c, and τ_d

Expressions of block i ($i = 3$–6) allow us to write the following three nonlinear equations:

$$\frac{\mathrm{Re}C\pi}{C_{bc} + Cc} + \frac{RbC}{C_{bc} + C_c} = b3 \tag{15}$$

$$Rb\left(\frac{C}{Cbc} + g0\frac{R_e C\pi}{Cbc + Cc}\right) = b5 \tag{16}$$

$$\frac{\mathrm{Re}C\pi}{(C_{bc} + C_c)}\frac{Rb\,C_{bc}}{(C_{bc} + C_c)} = \frac{b6 - L_e}{b4} \tag{17}$$

with $x = (C)/C_{bc}$, $y = R_b$, and $Z = (b6 - L_e)/(C_{bc} + C_c)$. Equations (15)–(17) can be rewritten as $Z + xy(1-x) = b3$, $y = R_b$, $y(x + g0z) = b5$, $Zy(1-x) = (b6 - L_e)/b4$, by naming $U = b3$, $V = b5$, and $W = (b6 - L_e)/b4$, we obtain

$$\frac{V}{W^2}z^2 + \left(\frac{1}{W} - \frac{UV}{W^2}\right)z + \left(\frac{V - U}{W} - g_0\right) = 0. \tag{18}$$

Using physical solution Z^+ of (18) and knowing the different blocks, we have $C_\pi = (Z + b4b7)/R_\pi$, $C_c = ((b4^2 Z^+(b3 - Z^+))/(b6 - L_c)$, and $C_{bc} = b4\Big[1 - (b4Z^+(b3 - Z^+))/(b6 - L_e)\Big]$, $R_b = (b6 - L_e)/\Big(b4Z^+\left(1 - (b4Z^+(b3 - Z^+))/(b6 - L_e)\right)\Big)$, $R_c = b1 - Z^+$, and $\tau_d = b4b3 - (b9 + L_c)/(Z^+)$

IV. Results and Discussion

The method is validated by investigating GaInP/GaAs and GaInP/InP HBTs at multibias conditions. The bias variation of the capacitances C_π and C_{bc}, shown in Fig. 2(c) and (d), agrees well with the prevision of physical analysis. The good regularity of the calculated capacitances demonstrates the unicity of the solution. Fig. 3 shows the measured and modeled S-parameters over a frequency range of 0.3–40 GHz. Good agreement in magnitude and phases is obtained. In particular, the evolution versus frequency of all the calculated S-parameters is the same as the measured ones.

V. Conclusion

We have demonstrated a new method to directly determine the HBT small-signal equivalent circuit. No use of numerical optimization, nor local fitting routines are required in the procedure. It uses the measured S-parameters to determine independently nine analytical expression blocks, which allow us to calculate the circuit elements. The procedure allows us to determine the base and collector resistances at each bias point with the other bias-dependent elements. In addition to the good agreement obtained between measured and simulated S-parameters of the HBT, the bias dependence of the base–emitter and base–collector capacitances obtained from the proposed multibias extraction procedure agrees well with the prevision of physical analysis.

References

[1] D. Costa, W. U. Liu, and J. S. Harris, "Direct extraction of the AlGaAs/GaAs heterojunction bipolar transistor small-signal equivalent circuit," *IEEE Trans. Electron Devices*, vol. 38, pp. 2018–2024, Sept. 1991.

[2] S. Lee and A. Gopinath, "Parameter extraction technique for HBT equivalent circuit using cutoff mode measurement," *IEEE Trans. Microwave Theory Tech.*, vol. 40, pp. 574–577, Mar. 1992.

[3] S. Lee, B. R. Ryum, and S. W. Kang, "A new parameter extraction technique for small-signal equivalent circuit of polysilicon emitter bipolar transistors," *IEEE Trans. Electron Devices*, vol. 41, pp. 233–238, Feb. 1994.

[4] S. J. Spiegel, P. R. Smith, D. R. Ritter, R. A. Hamm, A. Feygenson, and P. R. Smith, "Extraction of the Inp/GaInAs heterojunction bipolar transistor small-signal equivalent circuit," *IEEE Trans. Electron Devices*, vol. 42, pp. 1059–1064, June 1995.

[5] U. Schaper and B. Holzapfl, "Analytical parameter extraction of the HBT equivalent circuit with T-like topology from measured S-parameters," *IEEE Trans. Microwave Theory Tech.*, vol. 43, pp. 493–498, Mar. 1995.

[6] C. J. Wei and J. C. M. Hwang, "Direct extraction of equivalent circuit parameters for heterojunction bipolar transistor," *IEEE Trans. Microwave Theory Tech.*, vol. 43, pp. 2035–2040, Sept. 1995.

[7] A. Samelis and D. Pavlidis, "DC to high-frequency HBT-model parameter evaluation using impedance block conditioned optimization," *IEEE Trans. Microwave Theory Tech.*, vol. 45, pp. 886–897, 1997.

[8] B. Li, S. Prasad, L.-W. Yang, and S. C. Wang, "A semianalytical parameter-extraction procedure for HBT equivalent circuit," *IEEE Trans. Microwave Theory Techniques*, vol. 46, pp. 1427–1435, Oct. 1998.

[9] S. A. Maas and D. Tait, "Parameter extraction method for heterojunction bipolar transistors," *IEEE Trans. Microwave Guided Wave Lett.*, vol. 2, pp. 502—502, Dec. 1992.

[10] A. Ouslimani, J. Gaubert, H. Hafdallah, A. Birafane, P. Pouvil, and H. Leier, "New method for determining parasitic access inductances of high frequency on wafer coplanar heterojunction bipolar transistors," in *GAAS'98*, pp. 391–394.